Title

The AAA+ ATPase Msp1 is a processive protein translocase with robust unfoldase activity

Journal

Proceedings of the National Academy of Sciences of the United States of America, 117(26)

ISSN

0027-8424

Authors

Castanzo, Dominic T
LaFrance, Benjamin
Martin, Andreas

Publication Date

2020-06-30

DOI

10.1073/pnas.1920109117

Peer reviewed

The AAA+ ATPase Msp1 is a processive protein translocase with robust unfoldase activity

Dominic T. Castanzo[a,b], Benjamin LaFrance[a,b], and Andreas Martin[a,b,c,1]

[a]Department of Molecular and Cell Biology, University of California, Berkeley, CA 94720; [b]California Institute for Quantitative Biosciences, University of California, Berkeley, CA 94720; and [c]Howard Hughes Medical Institute, University of California, Berkeley, CA 94720

Edited by Stephen Bell, HHMI and Massachusetts Institute of Technology, Cambridge, MA, and approved May 16, 2020 (received for review November 14, 2019)

Msp1 is a conserved eukaryotic AAA+ ATPase localized to the outer mitochondrial membrane, where it is thought to extract mislocalized tail-anchored proteins. Despite recent in vivo and in vitro studies supporting this function, a mechanistic understanding of how Msp1 extracts its substrates is still lacking. Msp1's ATPase activity depends on its hexameric state, and previous characterizations of the cytosolic AAA+ domain in vitro had proved challenging due to its monomeric nature in the absence of the transmembrane domain. Here, we used a hexamerization scaffold to study the substrate-processing mechanism of the soluble Msp1 motor, the functional homo-hexameric state of which was confirmed by negative-stain electron microscopy. We demonstrate that Msp1 is a robust bidirectional protein translocase that is able to unfold diverse substrates by processive threading through its central pore. This unfoldase activity is inhibited by Pex3, a membrane protein proposed to regulate Msp1 at the peroxisome.

Msp1 | Pex3 | Pex15 | AAA+ ATPase

Msp1 (ATAD1 or Thorase in mammals) is an ATPase of the AAA+ (ATPases Associated with various cellular Activities) protein superfamily that resides in the outer mitochondrial membrane (OMM) and functions in protein quality control (1). Several in vivo studies demonstrated that Msp1's role for proteostasis lies in the extraction of mislocalized Tail Anchored (TA) proteins from the OMM (2, 3) as well as in the clearance of impaired or unimported mitochondrial precursor proteins at the translocase of the outer membrane (TOM) complex (4). Deleting components of the Guided Entrance of Tail-anchored proteins (GET) pathway, one of the systems responsible for proper localization of TA proteins, exaggerates mislocalization of some ER-destined TA proteins to the OMM, and additional deletion of Msp1 leads to the accumulation of these mislocalized proteins at mitochondria (2, 3, 5) and the development of growth defects (6). For clearing mitochondrial precursor proteins that failed to be imported into mitochondria, Msp1 is thought to cooperate with Cis1 and Tom70 of the TOM complex in the mitochondrial compromised protein import response (mitoCPR) pathway (4). Although Msp1's importance for proteostasis at the mitochondrial membrane is well established, the mechanisms used by this motor to extract its substrates remain elusive.

Recent in vivo studies have shown that Msp1-mediated protein extraction from mitochondria is dependent on ATP hydrolysis, and several putative substrates have been identified, including the essential peroxisomal TA protein Pex15 that is extracted by Msp1 when mislocalized to the OMM (2, 3). Cross-linking studies have implicated a short stretch of hydrophobic amino acids near the transmembrane domain (TMD) of Pex15 as Msp1's binding site, providing insight into how Msp1 may recognize substrates (7). Interestingly, Msp1 can also be found in the peroxisomal membrane, where Pex15 plays an essential role in peroxisome biogenesis and should therefore be spared from Msp1-mediated membrane extraction (8, 9). It was suggested that direct interaction with another peroxisomal membrane protein, Pex3, shields Pex15 at the peroxisome from recognition by Msp1 (10), but the mechanisms underlying this inhibition are unclear.

Previous functional studies of Msp1 in vitro had been limited by the fact that this ATPase does not form stable hexamers in the absence of its TMD, similar to other membrane-bound AAA+ motors (11, 12). Hexamers of $^{\Delta TMD}$Msp1 could only be stabilized when eliminating robust ATP hydrolysis, either in the presence of the slowly or nonhydrolyzable ATP analog ATPγS or upon mutation of Msp1's Walker B glutamate (6), which traps the motor in a permanent ATP-bound state and thus largely limits functional characterizations. Full-length Msp1 reconstituted into proteoliposomes was found to be capable of extracting model substrates from these liposomes in a manner dependent on ATP hydrolysis and the presence of conserved pore loops (6), which for other AAA+ hexamers have been shown to project from every subunit into the central pore to directly contact the substrate polypeptides for translocation (13). However, important outstanding questions include whether Msp1 extracts substrates via a tug-and-release mechanism or processive threading through its central pore, how it recognizes substrates, and how Pex3 inhibits the extraction of peroxisomal Pex15. Answering these questions will be instrumental in decrypting Msp1's role in the OMM and peroxisomal membrane.

In this study, we generated soluble $^{\Delta TMD}$Msp1 hexamers by fusing the cytosolic AAA+ ATPase domain to a hexamerization scaffold and thereby facilitating ring formation in vitro, which was confirmed by negative-stain electron microscopy (EM). Furthermore, we show that soluble hexameric Msp1 is a robust

Significance

The AAA+ ATPase Msp1 has previously been shown to function in the quality control of tail-anchored proteins at the mitochondrial and peroxisomal membranes, yet its detailed mechanisms of substrate processing have remained unknown. Using scaffolds to stabilize the functional hexamer of Msp1 ATPase domains and various model proteins derived from Msp1's endogenous substrate Pex15, we show that Msp1 is a promiscuous protein translocase that mechanically unfolds and pulls its substrates through the central pore of the ATPase hexamer in an N-to-C or C-to-N terminal direction. The peroxisomal protein Pex3 modulates Msp1's activity at the peroxisome by directly interacting with the AAA+ hexamer and inhibiting substrate threading.

Author contributions: D.T.C. and A.M. designed research; D.T.C. and B.L. performed research; D.T.C. contributed new reagents/analytic tools; D.T.C., B.L., and A.M. analyzed data; and D.T.C. and A.M. wrote the paper.

The authors declare no competing interest.

This article is a PNAS Direct Submission.

[1]To whom correspondence may be addressed. Email: a.martin@berkeley.edu.

This article contains supporting information online at https://www.pnas.org/lookup/suppl/doi:10.1073/pnas.1920109117/-/DCSupplemental.

First published June 15, 2020.

protein translocase capable of unfolding diverse substrates via processive threading through the central pore. Contrary to the previously proposed model, we find that Pex3 does not shield the Pex15 substrate, but directly interacts with the Msp1 motor and inhibits its unfolding activity.

Results

Reconstitution of Functional $^{\Delta TMD}$Msp1 Using Hexamerization Scaffolds. Similar to other AAA+ ATPases, Msp1 is believed to function as a hexamer. However, we and others observed that heterologously expressed $^{\Delta TMD}$Msp1 purifies as a mixture of monomers and dimers, as determined by size-exclusion chromatography and multi-angle light-scattering analysis (Fig. 1*B*) (6). At high concentrations, $^{\Delta TMD}$Msp1 shows low levels of ATP hydrolysis, which are lost again upon dilution (*SI Appendix*, Fig. S1*A*), suggesting low affinity between $^{\Delta TMD}$Msp1 protomers. In order to restore $^{\Delta TMD}$Msp1 activity in vitro, we therefore tested three different hexamerization scaffolds in place of Msp1's TMD: the N-terminal domain of the archaeal proteasome-activating nucleotidase (PAN) from *Methanocaldococcus jannaschii* (14), the de novo engineered coiled-coil ccHex (15), and the Hcp1 protein from *Pseudomonas aeruginosa* (16) (Fig. 1*A*). The PAN N-terminal domain, which forms a stable hexameric ring or N-ring (from hereon called PANN) has not yet been exploited as a hexamerization scaffold, whereas both ccHex and Hcp1 have previously been used to aid in stabilizing other homohexameric AAA+ ATPases (11, 17). Each of the fusion constructs with these domains appended to the N terminus of $^{\Delta TMD}$Msp1 eluted in size-exclusion chromatography at a similar volume as the ATP-bound Walker B mutant $^{\Delta TMD}$Msp1-E193Q, which is known to form hexamers under such conditions (Fig. 1*B*). To further assess the oligomeric state of these Msp1 fusions, we employed negative-stain EM. Two-dimensional (2D) class averages and three-dimensional (3D) reconstructions of PANN-Msp1, ccHex-Msp1, and Hcp1-Msp1 suggest that each construct forms homogeneous, hexameric particles with an ∼13-nm diameter (Fig. 1*C* and *SI Appendix*, Fig. S2 *A*–*C*), which is consistent with previously observed hexamers of ATPase-inhibited $^{\Delta TMD}$Msp1 Walker B mutants (6). Published structures of each isolated hexamerization scaffold could be docked into the corresponding densities of the 3D reconstructions (*SI Appendix*, Fig. S2*C*). The Msp1 motor showed similar conformations in all three constructs, with the ATPase domains forming a lock-washer or spiral staircase of five protomers and one less-resolved protomer at the seam (*SI Appendix*, Fig. S2*D*). Msp1 thus strongly resembles other AAA+ translocases (18), confirming that the fused hexamerization scaffolds had no effect on the overall ring conformation.

We subsequently tested these constructs for ATPase activity and observed robust hydrolysis for PANN-Msp1, ccHex-Msp1, and Hcp1-Msp1 at low concentrations. This is in stark contrast to the nonfused $^{\Delta TMD}$Msp1 (Fig. 1*D*), which even at 1.25 μM showed only 15% ATPase activity compared to the fusion constructs, indicating low affinity of the isolated protomers in the micromolar range (*SI Appendix*, Fig. S1*A*). Since all oligomerized constructs exhibited similar ATP-hydrolysis rates, we believe that the various scaffolding domains do not considerably affect Msp1's ATPase activity. Within the range of tested Msp1 concentrations, we did not observe a concentration dependence of the ATPase activity, indicating that the scaffolds mediate hexamer formation with at least nanomolar affinities (*SI Appendix*, Fig. S1 *A* and *B*).

Hexameric Msp1 Can Unfold Pex15 and Requires Long Unstructured Regions for Initiation. To determine whether Msp1 has unfoldase activity similar to many other AAA+ protein translocases, we used Pex15, a putative Msp1 substrate and TA peroxisomal membrane protein that occasionally mislocalizes to the OMM (2, 3). We had previously established the soluble portion of Pex15 for an unfoldase assay to characterize another AAA+ motor, Pex1/Pex6, where we took advantage of Pex15's cysteines being all buried when in the folded state (19). Upon unfolding, these cysteines become accessible for labeling with fluorescein-5-maleimide (F5M), which therefore also provides a robust approach to test Msp1's unfoldase activity (Fig. 2*A*).

We first tested a truncated construct of Pex15 lacking the N-terminal unstructured region as well as the C-terminal hydrophobic segment and transmembrane domain [Pex15$^{43\text{-}309}$ (19)]. Consistent with a lack of stable hexamerization, nonfused $^{\Delta TMD}$Msp1 showed no unfoldase activity even at high concentrations (Fig. 2*A*). In contrast, all three Msp1-fusion constructs were able to unfold Pex15, albeit to varying extents, with PANN-Msp1

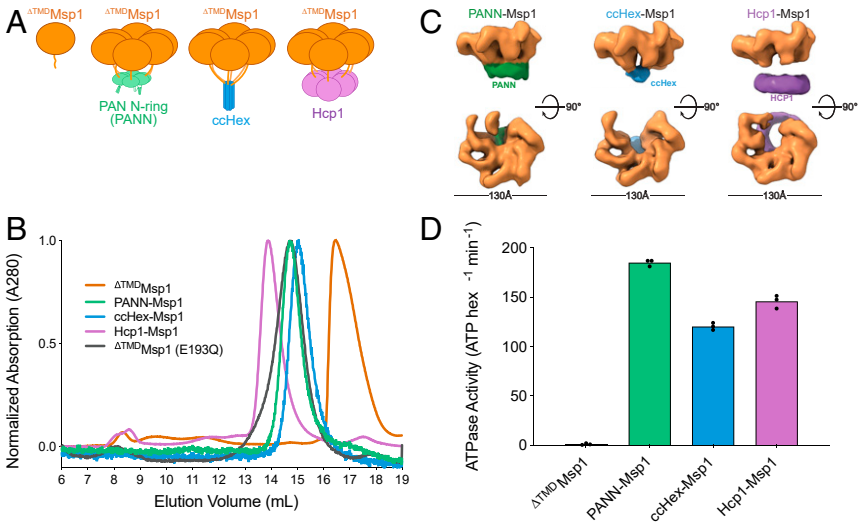

Fig. 1. N-terminally fused oligomerizing scaffolds facilitate hexamerization of $^{\Delta TMD}$Msp1. (*A*) Cartoon depiction of $^{\Delta TMD}$Msp fused to PANN, ccHex, and Hcp1. (*B*) Elution profiles from size-exclusion chromatography for PANN, ccHex, and Hsp1 fusions of $^{\Delta TMD}$Msp1 compared to $^{\Delta TMD}$Msp1 and $^{\Delta TMD}$Msp1^{E193Q}, indicating scaffold-induced oligomerization. (*C*) Three-dimensional class averages from negative-stain EM for each scaffold-Msp1 fusion construct reveal hexamers of the expected shape and size. (*D*) PANN-Msp1, ccHex-Msp1, and Hcp1-Msp1 possess robust ATPase activity in contrast to $^{\Delta TMD}$Msp1. Data reflect ATPase rates for 100 nM scaffolded Msp1 and 1,250 nM $^{\Delta TMD}$Msp1 (hexamer equivalents; $n = 3$, technical replicates).

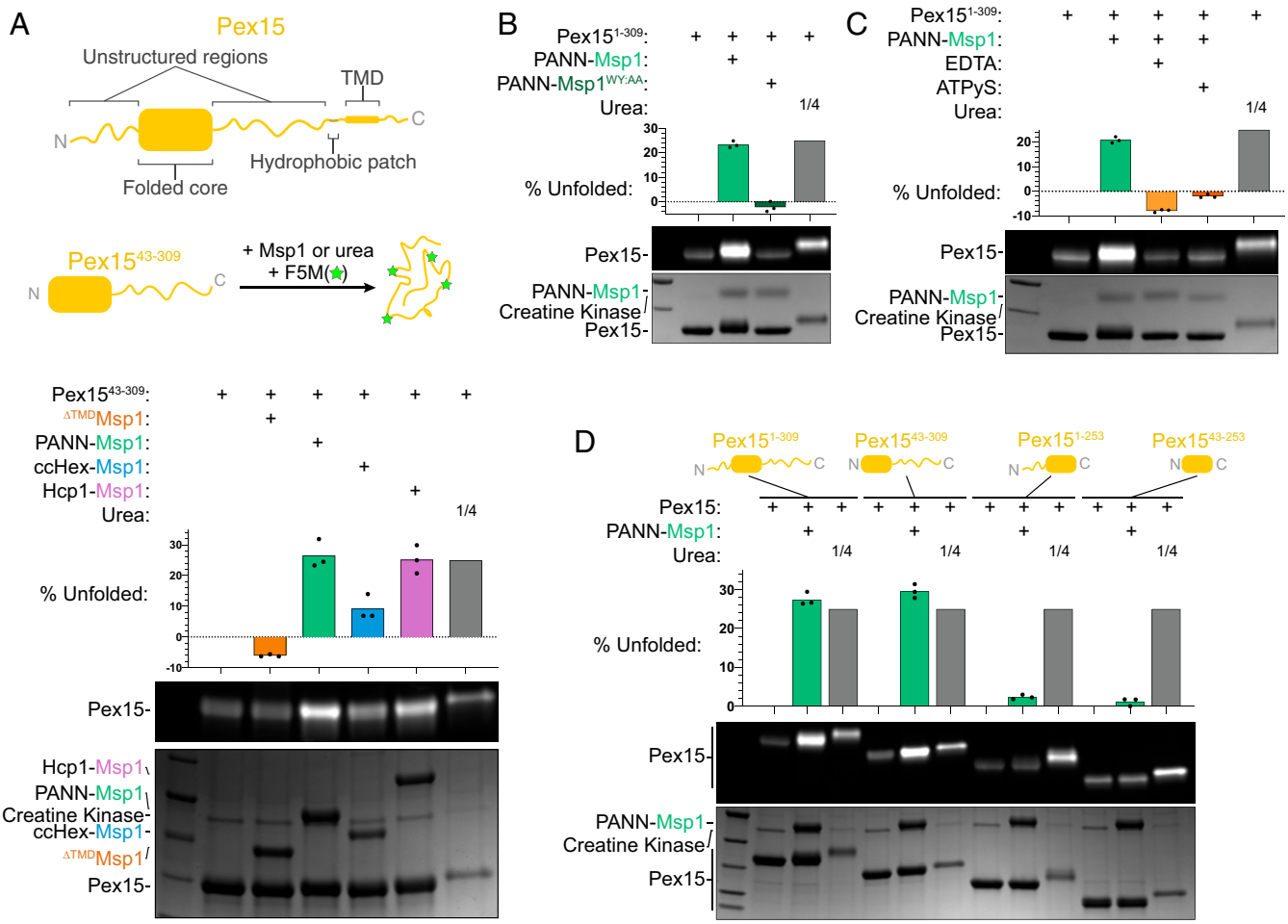

Fig. 2. Hexameric Msp1 is an unfoldase requiring long unstructured regions. (*A*,*Top*) Domain architecture of Pex15 and cartoon depiction of the maleimide-labeling–based unfoldase assay. Pex15 is incubated with Msp1 and then pulse-labeled with F5M before analysis by SDS-PAGE. (*Bottom*) SDS-PAGE analysis of the maleimide-labeling unfoldase assays for $^{\Delta TMD}$Msp1 and its scaffold fusions. The fluorescence scan for F5M-labeled Pex15 is shown at the top and the Coomassie Brilliant Blue stain to visualize every reaction component at the bottom. The last lane on the right represents a control reaction with Pex15 completely unfolded by urea prior to F5M labeling and one-fourth of the volume loaded compared to all other samples. (*B*) SDS-PAGE analysis as in *A* for Pex15 unfolding by PANN-Msp1 or its pore-1 loop mutant (W166A/Y167A). (*C*) SDS-PAGE analysis as in *A* for unfoldase reactions in the absence or presence of EDTA and ATPγS as inhibitors of ATP hydrolysis. (*D*) SDS-PAGE analysis as in *A* for unfoldase reactions of Pex15 model substrates with flexible regions of various lengths at the N or C termini, as indicated by the schematics above the gel. Only constructs containing Pex15's longer C-terminal unstructured region are unfolded by PANN-Msp1.

and Hcp1-Msp1 being notably better unfoldases than ccHex-Msp1 (Fig. 2*A*). Since ccHex-Msp1 and Hcp1-Msp1 yielded much less protein from recombinant expression, we chose the PANN fusion to further characterize Msp1's motor mechanism, and all assays henceforth were performed using this construct.

PANN-Msp1 exhibited processive unfoldase activity with linear steady-state kinetics of Pex15 unraveling over a 40-min reaction (*SI Appendix*, Fig. S3*A*). Since F5M labeling of accessible cysteines was performed for only 45 s after the 40-min incubation with Msp1, this steady increase of labeled substrate with increasing Msp1 incubation time indicates that the majority of Pex15 unfolds irreversibly or at least refolds with a rate that is much lower than the unfolding rate constant of Msp1. To confirm that this unfoldase activity originated from Msp1 and not a contaminating protein or the PANN scaffold itself, we mutated both pore-1 loop residues, W166 and Y167, to alanines (PANN-Msp1$^{WY:AA}$) and observed a complete loss of unfoldase activity (Fig. 2*B*), despite the persistence of stable hexamers and an increase in the rate of ATP hydrolysis (*SI Appendix*, Fig. S3*B*). This is consistent with previous studies that found Msp1's pore loops to be essential for substrate extraction from membranes in vitro and in vivo (6). Furthermore, the inhibition of unfoldase activity upon chelating Mg^{2+} ions with ethylenediaminetetraacetic acid (EDTA) or adding the non- or slowly hydrolyzable ATP analog ATPγS demonstrates that Msp1-mediated unfolding of Pex15 is an ATP-hydrolysis–dependent process (Fig. 2*C*). Although many other AAA+ motors respond to substrate processing with increased or decreased ATPase rates (19, 20), the ATPase activity of PANN-Msp1 remained unaffected by the addition of Pex15. The presence of substrate also failed to stimulate the extremely slow ATP hydrolysis by the nonfused $^{\Delta TMD}$Msp1, indicating that Msp1 hexamerization is, at least in vitro, not substrate-induced (*SI Appendix*, Fig. S3*C*).

Next, we explored the minimal substrate requirements of Msp1 unfoldase activity by using various Pex15 truncations (Fig. 2*D*). The structured core of Pex15 (Pex15$^{43-253}$) alone cannot be unfolded by PANN-Msp1, suggesting that the motor requires an unstructured segment to engage a substrate (Fig. 2*D*). The C-terminal flexible region, as present in Pex15$^{43-309}$, is sufficient for this engagement and Msp1-mediated unfolding, whereas the N-terminal tail, as present in Pex15$^{1-253}$, does not allow Pex15 processing unless it is extended by an additional 20 unstructured amino acids ($^{\wedge 20aa}$Pex15$^{1-253}$, *SI Appendix*, Fig. S3*D*). Hence, Pex15's

endogenous N-terminal tail is likely not long or flexible enough to reach the pore loops in Msp1 and consequently has no effects on the engagement of Pex15$^{1\text{-}309}$, which seems to occur solely through the C-terminal unstructured region (Fig. 2*D*).

Hexameric Msp1 Unfolds Substrates by Processively Threading through Its Central Pore. The extraction of mislocalized membrane proteins by Msp1 could occur in two possible ways: 1) via processive threading through the central pore or 2) via a tug-and-release mechanism. In order to distinguish between these two models, we exploited that Msp1 engages Pex15 from its C-terminal unstructured region and designed a fluorescent reporter substrate, mEOS-MBP-Pex15$^{1\text{-}309}$, the MBP and mEOS moieties of which would become unfolded only during processive substrate threading. MBP was included both to increase substrate solubility and to assess Msp1's unfolding capabilities. mEOS is a GFP-like photoactivatable protein whose backbone cleavage upon illumination at 405 nm causes a shift from green to red fluorescence (*SI Appendix*, Fig. S4*A*) (20, 21). The cleaved version maintains its 3D structure until unfolding irreversibly separates the two pieces, leading to a loss of red fluorescence. Monitoring the fluorescence of red mEOS, or mEOS(R), can thus be used in continuous unfolding assays to perform kinetic analysis of Msp1 activity.

Unfused mEOS(R) showed equally small fluorescence decreases in the absence and presence of PANN-Msp1 (Fig. 3*A*), indicating that Msp1 is unable to unfold mEOS when lacking an unstructured region for initiation. In contrast, mEOS(R)-MBP-Pex15$^{1\text{-}309}$ exhibited a considerable loss of fluorescence in the presence of PANN-Msp1, consistent with its ATP-dependent unfolding at a rate of ~0.12 motor^{-1}·min^{-1} (Fig. 3 *A* and *B*). Consistent with our previous results for the unfolding of unfused Pex15, we found that Msp1 was unable to unfold a mEOS-MBP-Pex15$^{1\text{-}253}$ variant lacking Pex15's C-terminal unstructured region. We can therefore conclude that the motor engages the full-length mEOS-MBP-Pex15$^{1\text{-}309}$ construct from the C-terminal unstructured region of Pex15 and processively threads the substrate to unfold multiple domains. This model is further supported by our results from the maleimide-labeling assay, in which we confirmed robust unfolding when mEOS-MBP-Pex15$^{1\text{-}309}$ was incubated with Msp1 under the same experimental conditions as for the fluorescence detection of mEOS unfolding (*SI Appendix*, Fig. S4*B*).

Having established the ability of Msp1 to processively thread and unfold multidomain substrates, we set out to evaluate the unfolding of another structured domain, SUMO, by inserting it between mEOS(R) and Pex15 and measuring the loss of mEOS(R) fluorescence. Compared to the equivalent MBP-containing substrate, the SUMO fusion was much more slowly unfolded by Msp1 (Fig. 3*C*). Using the maleimide-labeling assay, we observed that the Pex15 domain in mEOS-SUMO-Pex15$^{1\text{-}309}$ was unfolded with similar kinetics as in other fusion constructs (*SI Appendix*, Fig. S4*C*), indicating that indeed the SUMO domain represents the major, rate-determining unfolding barrier for this substrate, consistent with its considerable thermodynamic stability. Importantly, the extent of Pex15 labeling in this assay is consistent with multiple-turnover unfolding, which would be possible only if the mEOS-SUMO-Pex15$^{1\text{-}309}$ substrate is frequently released once Msp1 reaches the tough-to-unfold SUMO domain. Introducing the C52A mutation, which was previously shown to reduce the global stability of SUMO (22), did not significantly increase the rate for complete unfolding of mEOS-SUMO-Pex15$^{1\text{-}309}$ by Msp1 (*SI Appendix*, Fig. S4*D*), suggesting that this mutation has no effect on the local stability at SUMO's C terminus. In summary, our results for the Pex15 fusion substrates established that Msp1 is a promiscuous unfoldase, capable of unraveling various folded domains through processive threading starting at Pex15's unstructured C-terminal region.

Hexameric Msp1 Is a Promiscuous, Bidirectional Unfoldase. A recent study reported that a hydrophobic region near Pex15's C terminus (residues 313 to 324) is key to Msp1 recognition and engagement (7). In our isolated Pex15 model substrate we omitted this segment due to its drastic effect on solubility, but the solubility-increasing MBP moiety fused to Pex15 allowed us to characterize its effects on substrate recognition by Msp1. Interestingly, we observed no significant change in Pex15 unfolding upon incorporation of the hydrophobic region (*SI Appendix*, Fig.

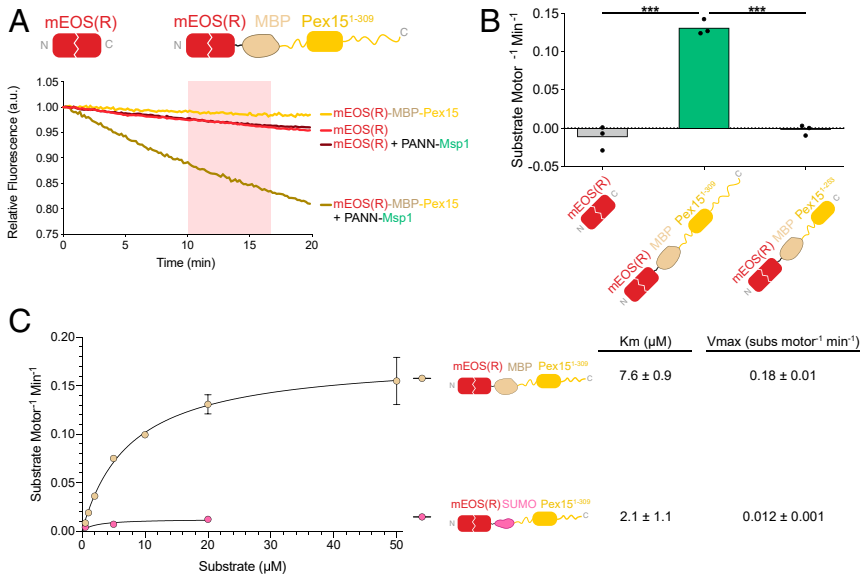

Fig. 3. Hexameric Msp1 can unfold consecutive folded domains via processive threading. (*A*) Representative traces showing loss of mEOS(R) fluorescence only for mEOS-MBP-Pex15 in the presence of PANN-Msp1. Time frame indicated by red shading was used to quantify unfolding kinetics, with rates reported in *B* (***$P < 0.001$; $n = 3$, technical replicates). (*C*) Michaelis–Menten kinetics reveal differences in K_m and V_{max} for mEOS(R)-Pex15 fusion substrates with MBP or SUMO insertions ($n = 3$, technical replicates; error bars represent SD).

S4*E*), indicating that, at least in vitro, it plays no major role for Msp1 binding or processing.

Msp1's cellular function in extracting mislocalized TA proteins suggests that it is able to recognize a diverse array of substrates. This is supported by previous observations for the Msp1-mediated proteoliposome extraction of model substrates, in which SUMO was fused to the TMD of Sec22 (6). To determine whether our reconstituted hexameric Msp1 retained this promiscuity in substrate selection, we tested its ability to engage and unfold a non-Pex15 substrate, mEOS(R)-IDR, where mEOS(R) is fused to a 68-amino-acid intrinsically disordered region (IDR) derived from Cyclin B (20, 23). Interestingly, PANN-Msp1 was able to unfold this substrate with similar efficiency as mEOS-MBP-Pex15$^{1\text{-}309}$ (Fig. 4*A*), supporting the model that Msp1 requires sufficiently long unstructured regions for engagement but otherwise exhibits poor substrate specificity.

Thus far, our data suggest that Msp1 unfolds substrates from a free C terminus. To test a potential preference in the directionality of substrate threading, we therefore compared the unfolding rates of Pex15 substrates containing the Cyclin B-derived IDR on either the C terminus (Pex15$^{43\text{-}253}$-IDR) or N terminus (IDR-Pex15$^{43\text{-}253}$). Msp1's ability to equally process both substrates demonstrates that it is a bidirectional unfoldase (Fig. 4*B*), similar to many other protein translocases of the AAA+ family (24, 25).

Unfolding of IDR-Pex15$^{43\text{-}253}$ in comparison with Pex15$^{1\text{-}309}$ was also used to more rigorously evaluate the contribution of the PANN hexamerization scaffold to the observed motor promiscuity. All three Msp1 fusion constructs, PANN-Msp1, ccHex-Msp1, and Hcp1-Msp1, exhibit the same trend in that Pex15$^{1\text{-}309}$ is unfolded more efficiently than IDR-Pex15$^{43\text{-}253}$ (*SI Appendix*, Fig. S5), indicating that these differences in substrate processing are a feature of the Msp1 motor domain, rather than a contribution of the scaffolding domains.

Pex3 Directly Inhibits Msp1 Unfoldase Activity. Although Msp1 is predominantly found in the OMM where it extracts, for example, mislocalizedmitochondrial Pex15, it has also been observed in the peroxisomal membrane (2). At the peroxisome, however, Pex15 should be spared from Msp1 extraction, as it fulfills the important role of recruiting Pex1/Pex6 for peroxisome biogenesis (8, 9). The peroxisomal protein Pex3 has been proposed to bind Pex15 and shield it from extraction by peroxisomal Msp1 (10). In order to characterize this protective interaction, we expressed and purified the cytosolic portion of Pex3 (residues 40 to 441) fused to MBP for increased solubility (MBP-Pex3). As expected, MBP-Pex3 inhibited Pex15$^{1\text{-}309}$ unfolding by Msp1 (Fig. 5*A*). Our pulldown assays, however, revealed that there was no direct interaction between MBP-Pex3 and Pex15$^{1\text{-}309}$, whereas MBP-Pex3 bound hexameric PANN-Msp1 (Fig. 5*B* and *SI Appendix*, Fig. S7*A*). Pulldown controls with MBP and PANN alone confirmed that this interaction is indeed mediated by the cytosolic Msp1 and Pex3 domains (*SI Appendix*, Fig. S7 *C* and *D*). MBP-Pex3 was able to pull down Pex15$^{1\text{-}309}$ only in the presence of PANN-Msp1 (Fig. 5*B*), suggesting that Msp1 can simultaneously interact with both MBP-Pex3 and Pex15$^{1\text{-}309}$. Given these results, we hypothesized that Pex3 might inhibit Msp1 directly, rather than interacting with and shielding Pex15, and should therefore also be able to inhibit the unfolding of other, non-Pex15 substrates. Indeed, we found that MBP-Pex3 inhibited unfolding of mEOS-MBP-Pex15$^{1\text{-}309}$ and mEOS(R)-IDR to a similar extent (Fig. 5*C*), and with an IC50 of ~6.8 μM (Fig. 5*D*).

To confirm that Pex3 is a specific inhibitor of Msp1 and does not generally interfere with AAA+ motor function, we compared its effects on PANN-Msp1 and Pex1/Pex6. While MBP-Pex3 robustly inhibited Msp1-mediated unfolding of Pex15$^{1\text{-}309}$ and IDR-Pex15$^{1\text{-}253}$ in our maleimide-labeling assay (Fig. 5*E* and *SI Appendix*, Fig. S6*A*), substrate unfolding by Pex1/Pex6 proceeded unimpeded (Fig. 5*E*). This selective inhibition of Msp1 does not originate from an interference with ATP hydrolysis. At saturating concentrations of MBP-Pex3, we observed only a subtle 8% decrease of PANN-Msp1's ATPase activity (*SI Appendix*, Fig. S6*B*), which cannot account for the extent of unfoldase inhibition.

To dissect MBP-Pex3's interaction with the motor, we performed pull-down assays with either wild-type PANN-Msp1 or the pore loop mutant. Interestingly, MBP-Pex3 binding was strictly dependent on intact pore loops (*SI Appendix*, Fig. S7*B*), suggesting that this inhibitor binds in the central pore similarly to a substrate. In our maleimide unfoldase assay, incubation with Msp1 did not further increase the already substantial labeling of Pex3-intrinsic cysteines in the absence of the motor (*SI Appendix*, Fig. S7*E*), and insufficient solubility hindered the use of Pex3 fusions with mEOS to assess whether the inhibitor can be

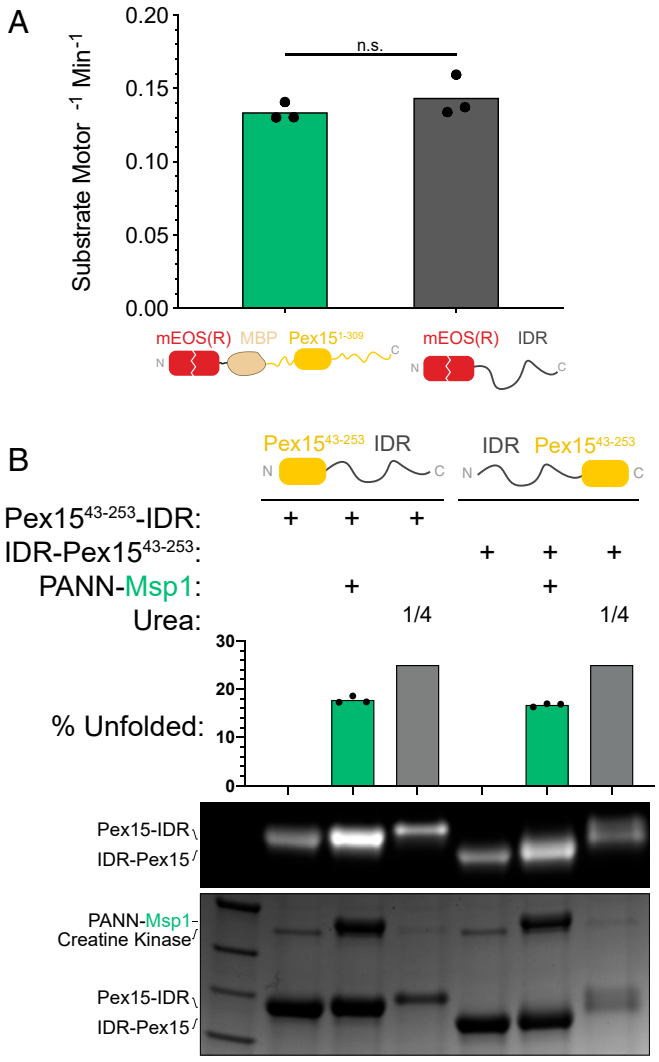

Fig. 4. Hexameric PANN-Msp1 is a robust and promiscuous unfoldase. (*A*) Rates for PANN-Msp1 unfolding of mEOS-MBP-Pex15 and mEOS-IDR ($n = 3$, technical replicates; n.s., not significant; $P = 0.35$). (*B*) SDS-PAGE analysis of the maleimide-labeling assay for the PANN-Msp1 unfolding of IDR-Pex15 and Pex15-IDR, demonstrating a lack of directionality in Msp1 threading. The fluorescence scan for F5M-labeled Pex15 is shown at the *Top*; the Coomassie Brilliant Blue stain to detect all reaction components is shown at the *Bottom*. The fourth and seventh lane show positive controls for complete Pex15 labeling after urea unfolding, with one-fourth of the volume loaded compared to all other reactions.

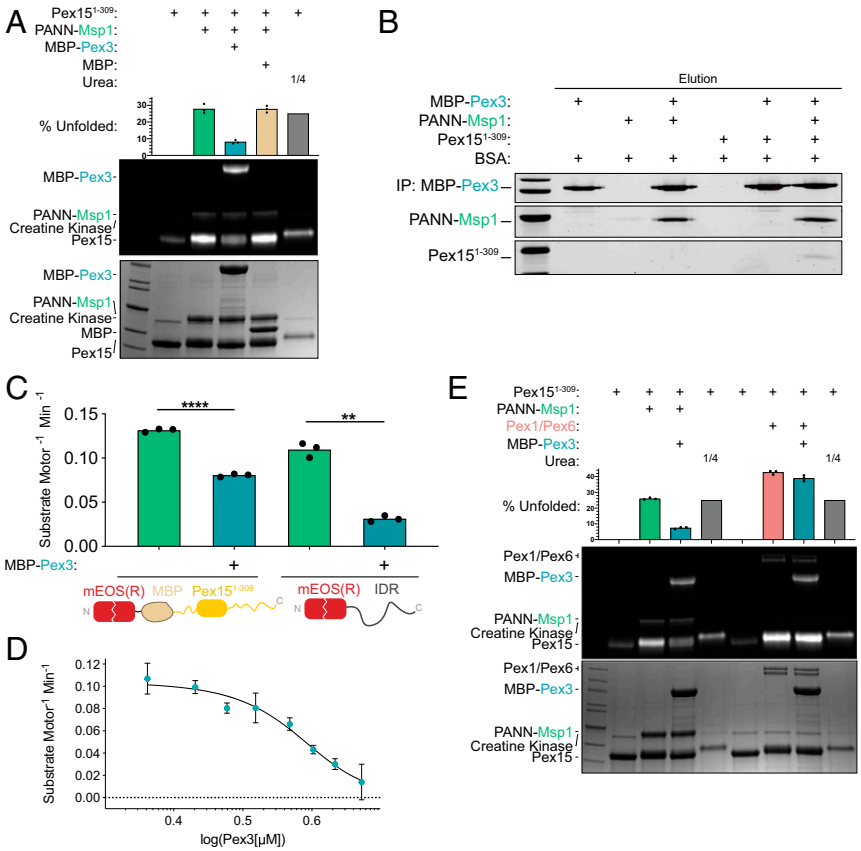

Fig. 5. Pex3 inhibits Msp1 unfoldase activity by directly binding to Msp1. (*A*) MBP-Pex3, but not MBP alone, inhibits PANN-Msp1's unfoldase activity. Shown is the SDS-PAGE analysis of the maleimide-based unfoldase assay with the fluorescence scan for F5M labeling at the top and the Coomassie Brilliant Blue stain at the bottom. (*B*) Coomassie Brilliant Blue-stained SDS-PAGE gel showing the pull-down of MBP-Pex3 with PANN-Msp1 or PANN-Msp1 and Pex15, but no interaction with Pex15 alone. (*C*) Rates for PANN-Msp1 unfolding of mEOS-MBP-Pex15 and mEOS-IDR substrates in the absence and presence of MBP-Pex3 ($n = 3$, technical replicates; $^{**}P < 0.005$, $^{****}P < 0.0001$). (*D*) Rates for mEOS-IDR unfolding by PANN-Msp1 in the presence of increasing concentrations of MBP-Pex3 inhibitor, revealing an IC50 of 6.8 μM ($n = 3$, technical replicates). (*E*) SDS-PAGE analysis of the maleimide-based assay for Pex15 unfolding by PANN-Msp1 and Pex1/Pex6 in the absence or presence of MBP-Pex3. MBP-Pex3 inhibits PANN-Msp1, but not Pex1/Pex6.

unfolded and threaded or potentially clogs the Msp1 motor. The detailed mechanisms for Pex3 inhibition of Msp1 therefore remain unclear. Nevertheless, our data provide strong evidence that the cytosolic domain of Pex3 does not interact with Pex15, but directly binds and inhibits Msp1.

Discussion

Detailed analyses of Msp1's structure and mechanisms have so far been hindered by the fact that its isolated, hydrolysis-active ATPase domain does not form stable hexamers in vitro. Here, we present a strategy to constitute functional Msp1 hexamers by fusing $^{\Delta TMD}$Msp1 to several hexameric scaffolds. Negative-stain EM revealed that each hexamerization strategy yields discrete Msp1 hexamers of the expected shape and size, and ATPase measurements confirmed robust hydrolysis activities that were unaffected by the fused scaffolds.

It had previously been unclear whether Msp1 functions by a tug-and-release mechanism or is able to thread and unfold substrates in a processive manner. We show that hexameric Msp1 is a robust bidirectional unfoldase that requires a long unstructured region for substrate engagement, but is capable of unfolding a variety of folded domains. Msp1's demonstrated ability to engage diverse IDRs is consistent with its in vivo role in extracting a multitude of peroxisomal, ER, Golgi, and plasma membrane TA proteins that were mislocalized to the mitochondrial membrane (2, 3, 7). It is unknown, however, whether an IDR of certain minimum length is merely a requirement of our reconstituted system, in which the N-ring of PAN sits above the entrance to the motor pore, or whether such flexible regions are also necessary for substrates processed by membrane-anchored Msp1.

We showed that hexameric Msp1 can unfold consecutive, linearly fused folded domains through processive threading, which is driven by its pore loops. Given its role in extracting TA proteins from membranes, Msp1's ability to translocate polypeptides in an N- to C-terminal direction may be particularly relevant to its in vivo function. However, we are unable to conclude whether Msp1's unfoldase activity is essential for substrate extraction during the quality control of TA proteins or in the mitoCPR pathway. One possible mechanism of extraction is that hexameric, closed-ring Msp1 engages an unstructured loop of the substrate near the TMD and then pulls on one strand of the loop to extract the TMD out of the membrane before either translocating the second strand to unfold structured domains from the C terminus or laterally releasing the substrate without further translocation and unfolding. Alternatively, individual Msp1 subunits or a split-open hexameric ring could encircle a membrane-anchored substrate and, once fully hexamerized, translocate in a N- to C-terminal direction to extract only the TMD. Although our reconstituted system allowed a detailed characterization of Msp1's unfoldase activity, exploring this motor's mechanism for the extraction of membrane proteins will require a deeper understanding of its oligomerization dynamics and substrate interactions in the membrane.

Our data provide important insight into the regulation of Msp1 at the peroxisomal membrane, where the cytosolic domain of Pex3 appears to prevent the extraction of Pex15 through direct binding and inhibition of Msp1, rather than shielding Pex15 as previously proposed. Importantly, Pex3 showed no effect on the unfoldase activity of Pex1/Pex6, which functions in close proximity to Pex3 at the peroxisomal membrane. A critical outstanding question therefore remains about the function of Msp1 in the peroxisomal membrane and how its inhibition by Pex3 may be modulated. It is possible that Pex15 and Pex3 are localized near the importomer, where Pex15 performs an important function in recruiting Pex1/Pex6 to the peroxisomal membrane and Pex3 may protect it from Msp1, whereas Msp1 functions as an extractase in the quality control of TA proteins elsewhere in the peroxisome. Extensive studies will be necessary to further elucidate Msp1's role at the peroxisome, as well as the factors that govern the selection of extraction-destined substrates.

Materials and Methods

Msp1 and Pex1/Pex6 Expression and Purification. The $^{\Delta TMD}$Msp1 construct corresponds to Msp1$^{36-362}$. The hexamerization scaffolds PAN N-domain (GenScript), ccHex (GenScript), and Hcp1 (Addgene, #87737) were fused to the N terminus of Msp1$^{36-362}$ with linkers that were five, nine, and six amino acids long, respectively, and contained alternating glycine and serine residues. All constructs contained a N-terminal 6xHis tag followed by a PreScission Protease cleavage site. Wild-type Msp1 constructs were expressed in *Escherichia coli* BL21*T1R cells in Terrific Broth (Novagen). Cultures were grown shaking at 37 °C until induction at $OD_{600} \sim 0.6$ with 0.1 mM isopropyl β-D-1-thiogalactopyranoside (IPTG; GoldBio). After expression for 3 to 4 h at 25 °C, cells were harvested by centrifugation at 6,000 × *g* for 20 min at 24 °C and then resuspended in Ni_A buffer (25 mM HEPES, pH 7.6, 100 mM NaCl, 100 mM KCl, 10 mM $MgCl_2$, 20 mM imidazole, 10% glycerol, 1 mM ATP, 0.5 mM EDTA) supplemented with leupeptin, pepstatin, aprotinin, 2 mg·mL^{-1} lysozyme, and benzonase (Novagen). Resuspended cell pellets were stored at −80 °C until thawed for purification. Cells were sonicated in ice water for 3 min (15 s on, 45 s off, 65% amplitude) before clarification centrifugation at 19,000 × *g* for 30 min at 4 °C. The supernatant was then allowed to batch bind to Ni-NTA resin for 30 min at 4 °C, rotating end over end. The resin was washed with ∼40 column volumes of Ni_A buffer before elution with 10 column volumes of room-temperature Ni_B buffer (Ni_A buffer with 250 mM imidazole and 5 mM ATP). The purification tags were subsequently cleaved off using 0.01 mg·mL^{-1} PreScission Protease during a 10-min incubation at room temperature. Cleaved eluates were concentrated using a 30 kDa molecular weight cut-off (MWCO) ($^{\Delta TMD}$Msp1) or 100 kDa MWCO (all PANN, ccHex, and Hcp1 fusions) concentrator (Amicon), filtered through a 0.22-μm filter, and further purified by size exclusion chromatography using a Superose 6 increase column (GE Life Sciences) in SEC buffer (50 mM HEPES, 50 mM NaCl, 50 mM KCl, 10 mM $MgCl_2$, 100 mM imidazole, 5% glycerol, 1 mM ATP, 0.5 mM EDTA). Fractions corresponding to the Msp1 hexamers (with peaks between 13.75 and 15.00 mL elution volume, depending on the scaffold) were then concentrated using a 100 kDa MWCO concentrator. The PANN-Msp1 pore loop mutant contained the W166A and Y167A mutations. The $^{\Delta TMD}$Msp1 harboring the Walker B mutation (E193Q) was purified in the absence of $MgCl_2$ and ATP and was mixed with SEC buffer immediately prior to injection into SEC. Pex1/Pex6 was expressed and purified as previously describe by Gardner et al. (19). All motor constructs were quantified using a Bradford assay and a bovine serum albumin (BSA; Sigma Aldrich) standard curve.

Pex15, mEOS, and Pex3 Protein Expression and Purification. All Pex15-, mEOS-, and Pex3$^{40-441}$-containing proteins were expressed in *E. coli* BL21*T1R cells grown in DYT (double yeast tryptone) media. Cultures were grown shaking at 37 °C and were induced at $OD_{600} \sim 0.6$ by the addition of $C_f = 0.3$ mM IPTG. Cultures were then grown at 18 °C overnight. These proteins were purified similarly to the Msp1 constructs, except that the Ni_A, Ni_B, and SEC buffers did not contain any ATP and the SEC buffer contained only 20 mM imidazole. Pex15- and mEOS-containing substrates included C-terminal FLAG-6xHis tags and were purified by Ni-NTA affinity chromatography. Tags were cleaved off (unless otherwise stated) using 0.01 mg·mL^{-1} PreScission Protease during a 10-min incubation period at room temperature after elution from Ni-NTA resin. For the experiments performed in *SI Appendix*, Fig. S4*E*, the C-terminal FLAG-6xHis tags on MBP-Pex15$^{1-309}$ and MBP-Pex15$^{1-327}$ were not cleaved off to maintain solubility. MBP-Pex3 was purified via an N-terminal 6xHis tag, which was removed with PreScission Protease as well. Additionally, each construct was further purified via size exclusion chromatography using a Superdex 200 increase column (GE Life Sciences). All non-Msp1 proteins were quantified by absorbance measurements at 280 nm. To generate red-fluorescent versions of mEOS-containing substrates, they were illuminated with a 405-nm laser set to 50 mV in 12 cycles of 2-min on-and-off intervals. The Cyclin B-derived IDR is composed of the following amino acid sequence: AHGGKHTFNNENVSARLGGACSIAVQAPAQHTFNNENVSARLGGALSIAVQAPAQSGSGSGS. The underlined sequence of 20 amino acids was also used to extend the N terminus of Pex15$^{1-253}$ for experiments presented in *SI Appendix*, Fig. S3*D*.

Fraction mEOS(R) protein is the quotient of the concentration of red mEOS (determined by A570) and the concentration of total protein (determined by A280). Extinction coefficients for all constructs were calculated using Benchling's Analysis of Translation tool (ExPASy).

ATPase Assays. ATPase activity was observed using an ATP/NADH-coupled enzyme assay where the regeneration of hydrolyzed ATP is coupled to NADH oxidation (26). All measurements were performed at 30 °C with reactions containing 10 μM BSA, 100 nM Msp1 hexamer (unless otherwise stated), and 20 μM substrate (Pex15$^{1-309}$, if included), as well as the coupled enzyme reaction mixture components 3 U·mL^{-1} pyruvate kinase, 3 U·mL^{-1} lactate dehydrogenase, 1 mM NADH, and 7.5 mM phosphoenolpyruvate. Concentrations of $^{\Delta TMD}$Msp1 are reported as hexamer equivalents. The absorbance of NADH was measured at 340 nM in a 96-well plate using a SpectraMAX 190 plate reader. Rate of hydrolysis was calculated using a 100-s window of steady-state activity (between 300 and 400 s after reaction start).

Negative-Stain Electron Microscopy. All Msp1 hexamers were diluted to 150 nM using EM Buffer (25 mM HEPES, pH 7.5, 50 mM NaCl, 50 mM KCl, 5 mM $MgCl_2$, 0.5 mM EDTA, 1 mM ATPγS) on ice. Samples were incubated at 24 °C for 2.5 min immediately before applying to the grid. Four microliters of each construct was placed on a 400-mesh continuous carbon grid that had been glow discharged (Tergeo, Pie Scientific). After adsorption of the sample onto the grid (2 min at room temperature), the sample was stained in five successive rinses with 40-μL droplets of Uranyl Formate (2% wt/vol in water). Grids were side-blotted with Whatman filter paper for 2 s and air dried for 5 min. Msp1 constructs were then visualized with an FEI Tecnai F20 electron microscope operating at 120 keV. For each construct, ∼150 micrographs were collected on an Ultrascan 4 k CCD camera (Gatan) at a magnification of 80,000× (1.37 Å/pixel) and a defocus range from −0.7 to −1.8 μm.

Each dataset was processed identically using relion/3.0.6 (27). Briefly, a contrast transfer function (CTF) estimation was performed using CtfFind4.1 (28), and particles were picked using relion's built-in Laplacian-of-Gaussian autopicker. Roughly 100-k particles were extracted for each dataset, binned fourfold, followed by 2D classification into 40 classes. All 2D classes that resembled hexameric protein complexes were selected to undergo 3D classification, and the two most abundant 3D classes were selected for the final refinement without imposing symmetry (∼40 k particles). To prevent model bias, a 13-nm Gaussian blob was used as the reference for 3D classification and refinement.

Maleimide-Labeling Unfoldase Assays. Maleimide-labeling reactions were performed using fluorescein-5-maleimide (Anaspec). Substrate proteins were used at a final concentration of 20 μM, and Msp1 constructs were used at a final concentration of 1 μM hexamer, unless otherwise stated. Each reaction also contained an ATP regeneration mixture (5 mM ATP, 0.03 mg·ml^{-1} creatine kinase, 16 mM creatine phosphate). Substrate proteins were diluted in Buffer_1 (50 mM HEPES, pH 7.5, 10 mM NaCl, 10 mM KCl, 10 mM $MgCl_2$, 0.5 mM EDTA), and Msp1 constructs were diluted in Buffer_1 + ATP regeneration mix. If included, MBP-Pex3 was added at a final concentration of 10 μM. Following addition of Msp1, reactions were incubated at 30 °C for 40 min before the addition of 250 μM F5M. In reactions including Pex1/Pex6, the ATPase was added at a final concentration of 0.25 μM and incubated at 30 °C for 5 min before the addition of 250 μM F5M. In specified experiments, 20 mM EDTA or 5 mM ATPγS was included. Reactions were incubated at 30 °C for 45 s and then quenched with an equal volume of 2× sodium dodecyl sulfate-polyacrylamide gel electrophoresis (SDS-PAGE) Sample Buffer (125 mM Tris, pH 6.8, 4% SDS, 20% glycerol, 0.01% bromophenol blue, 10% β-mercaptoethanol). To assess complete labeling of cysteines, "urea samples" were prepared by mixing the reaction components with buffer_2 (50 mM HEPES, pH 7.5, 10 mM NaCl, 10 mM KCl, 10 mM $MgCl_2$, 0.5 mM EDTA, 8 M urea) to reach a final urea concentration of 6 M. These samples were incubated in the presence of urea and 250 μM F5M at 30 °C for 40 min before 1:4 dilution with 2× SDS-PAGE Sample Buffer to quench the

reactions. All samples were boiled at 95 °C for 5 min prior to loading into a precast 4 to 20% acrylamide Mini-PROTEAN TGX gel (BioRad). Each reaction was performed in technical triplicates. Gels were imaged by fluorescein fluorescence detection using a ChemiDoc MP Imaging System (BioRad) and a Typhoon Trio Variable Mode Imager (GE Healthcare) before staining in Coomassie Brilliant Blue. On the Typhoon Trio Variable Mode Imager with the Typhoon Scanner Control v5.0 software (GE Healthcare), gels were imaged using a 520 BP 40 Cy2, ECL+, Blue FAM (488 nm) emission filter with a pixel size of 50 μm, and images were quantified with ImageQuant TL's 1D gel analysis toolbox (GE Healthcare Life Sciences) using automatic peak detection and background subtraction. For each construct, the resulting fluorescence value for the substrate-alone sample was subtracted from all experimental and control intensities. Urea control samples were multiplied by 4, to correct for the pre-PAGE dilution. The percentage of substrate unfolded was calculated by setting the substrate-alone fluorescence to 0% and the urea-containing sample to 100%.

mEOS Unfoldase Assays. mEOS fluorescence-based unfoldase assays were performed using 20 μM substrate, 1 μM Msp1 hexamer, 10 μM BSA, and ATP regeneration mixture. Substrate, BSA, and ATP regeneration mix were diluted in Buffer_1 prior to the addition of Msp1. When included, MBP-Pex3 was present at a final concentration of 10 μM unless otherwise stated. Following Msp1 addition, the reaction plate was loaded into a CLARIOstar Plus plate reader (BMG Labtech). Fluorescence emission at 588 nm (±20 nm, low pass filter of 561.2 nm) after excitation at 537 nm (±15 nm) was monitored for 20 min at 30 °C. Data were collected using the instrument's Installation Package V5.60 software before exporting via the MARS V3.10 software. Each reaction was performed in triplicate, and unfoldase rates were calculated from the steady-state slopes of each replicate, corrected for fact that only 10 to 40% of mEOS substrates were activated to form mEOS(R). Substrate-only experiments were also performed in triplicate, with their average rate being subtracted from each Msp1-containing replicate. Example raw data reported in Fig. 3*C* were normalized to the first value. Statistical analyses were done using Prism 8 (GraphPad) to perform an unpaired *t* test with Welch's correction.

Pulldowns. MBP-Pex3 (2 μM), Msp1 hexamers (1.67 μM), BSA (10 μM), $Pex15^{1\text{-}309}$ (10 μM), and ATP regeneration mix (ATP, creatine kinase, creatine phosphate) were coincubated in Buffer_3 for 5 min at 24 °C before an input aliquot was taken. The remaining reaction volume was added to prewashed Amylose Magnetic Resin (New England BioLabs). After incubation at 24 °C for 10 min, a flow-through sample was recovered before the resin was washed with Buffer_3 (50 mM HEPES, pH 7.5, 10 mM NaCl, 10 mM KCl, 10 mM $MgCl_2$, 0.5 mM EDTA, 1 mM ATP) and eluted with Buffer_3 + 10 mM maltose. Samples were mixed with an equal volume of 2× SDS/PAGE Sample Buffer and loaded onto a precast 4 to 20% acrylamide Mini-PROTEAN TGX Stain-Free gel (BioRad). Gels were imaged in the stain-free channel using a ChemiDoc MP Imaging System (BioRad) after 5 min UV activation. Pulldowns for the comparison of wild-type and pore-loop mutant Msp1 (*SI Appendix*, Fig. S7*B*) were stained with Coomassie Brilliant Blue to avoid differential detection by the stain-free method due to the elimination of tryptophans in the pore loop mutant.

Data Availability. All data are included in the manuscript and *SI Appendix*, and the experimental protocols outlined in *Materials and Methods* are sufficient to reproduce the work. Physical materials (e.g., strains and plasmids) will be made available upon reasonable request.

ACKNOWLEDGMENTS. We thank all members of the A.M. laboratory for contributions to experiment design, data analysis and interpretation, and useful discussions. A.M. is an HHMI investigator. This work was funded by the HHMI and by NIH Grant R01-GM0944 (to A.M.).

1. M. Nakai, T. Endo, T. Hase, H. Matsubara, Intramitochondrial protein sorting. Isolation and characterization of the yeast MSP1 gene which belongs to a novel family of putative ATPases. *J. Biol. Chem.* **268**, 24262–24269 (1993).
2. V. Okreglak, P. Walter, The conserved AAA-ATPase Msp1 confers organelle specificity to tail-anchored proteins. *Proc. Natl. Acad. Sci. U.S.A.* **111**, 8019–8024 (2014).
3. Y. C. Chen *et al*., Msp1/ATAD1 maintains mitochondrial function by facilitating the degradation of mislocalized tail-anchored proteins. *EMBO J.* **33**, 1548–1564 (2014).
4. H. Weidberg, A. Amon, MitoCPR-A surveillance pathway that protects mitochondria in response to protein import stress. *Science* **360**, eaan4146 (2018).
5. M. Schuldiner *et al*., The GET complex mediates insertion of tail-anchored proteins into the ER membrane. *Cell* **134**, 634–645 (2008).
6. M. L. Wohlever, A. Mateja, P. T. McGilvray, K. J. Day, R. J. Keenan, Msp1 is a membrane protein dislocase for tail-anchored proteins. *Mol. Cell* **67**, 194–202.e6 (2017).
7. L. Li, J. Zheng, X. Wu, H. Jiang, Mitochondrial AAA-ATPase Msp1 detects mislocalized tail-anchored proteins through a dual-recognition mechanism. *EMBO Rep.* **20**, e46989 (2019).
8. Y. Elgersma *et al*., Overexpression of Pex15p, a phosphorylated peroxisomal integral membrane protein required for peroxisome assembly in S.cerevisiae, causes proliferation of the endoplasmic reticulum membrane. *EMBO J.* **16**, 7326–7341 (1997).
9. I. Birschmann *et al*., Pex15p of Saccharomyces cerevisiae provides a molecular basis for recruitment of the AAA peroxin Pex6p to peroxisomal membranes. *Mol. Biol. Cell* **14**, 2226–2236 (2003).
10. N. R. Weir, R. A. Kamber, J. S. Martenson, V. Denic, The AAA protein Msp1 mediates clearance of excess tail-anchored proteins from the peroxisomal membrane. *eLife* **6**, e28507 (2017).
11. H. Shi, A. J. Rampello, S. E. Glynn, Engineered AAA+ proteases reveal principles of proteolysis at the mitochondrial inner membrane. *Nat. Commun.* **7**, 13301 (2016).
12. W. Peng *et al*., Structural insights into the unusually strong ATPase activity of the AAA domain of the Caenorhabditis elegans fidgetin-like 1 (FIGL-1) protein. *J. Biol. Chem.* **288**, 29305–29312 (2013).
13. A. Martin, T. A. Baker, R. T. Sauer, Pore loops of the AAA+ ClpX machine grip substrates to drive translocation and unfolding. *Nat. Struct. Mol. Biol.* **15**, 1147–1151 (2008).
14. F. Zhang *et al*., Structural insights into the regulatory particle of the proteasome from Methanocaldococcus jannaschii. *Mol. Cell* **34**, 473–484 (2009).
15. N. R. Zaccai *et al*., A de novo peptide hexamer with a mutable channel. *Nat. Chem. Biol.* **7**, 935–941 (2011).
16. J. D. Mougous *et al*., A virulence locus of Pseudomonas aeruginosa encodes a protein secretion apparatus. *Science* **312**, 1526–1530 (2006).
17. N. Monroe, H. Han, P. S. Shen, W. I. Sundquist, C. P. Hill, Structural basis of protein translocation by the Vps4-Vta1 AAA ATPase. *eLife* **6**, e24487 (2017).
18. S. N. Gates, A. Martin, Stairway to translocation: AAA+ motor structures reveal the mechanisms of ATP-dependent substrate translocation. *Protein Sci.* **29**, 407–419 (2020).
19. B. M. Gardner *et al*., The peroxisomal AAA-ATPase Pex1/Pex6 unfolds substrates by processive threading. *Nat. Commun.* **9**, 135 (2018).
20. M. M. Olszewski, C. Williams, K. C. Dong, A. Martin, The Cdc48 unfoldase prepares well-folded protein substrates for degradation by the 26S proteasome. *Commun. Biol.* **2**, 29 (2019).
21. M. Zhang *et al*., Rational design of true monomeric and bright photoactivatable fluorescent proteins. *Nat. Methods* **9**, 727–729 (2012).
22. H. Drobecq *et al*., A central cysteine residue is essential for the thermal stability and function of SUMO-1 protein and SUMO-1 peptide-protein conjugates. *Bioconjug. Chem.* **27**, 1540–1546 (2016).
23. J. A. M. Bard, C. Bashore, K. C. Dong, A. Martin, The 26S proteasome utilizes a kinetic gateway to prioritize substrate degradation. *Cell* **177**, 286–298.e15 (2019).
24. W. Piwko, S. Jentsch, Proteasome-mediated protein processing by bidirectional degradation initiated from an internal site. *Nat. Struct. Mol. Biol.* **13**, 691–697 (2006).
25. T. A. Baker, R. T. Sauer, ClpXP, an ATP-powered unfolding and protein-degradation machine. *Biochim. Biophys. Acta* **1823**, 15–28 (2012).
26. J. G. Nørby, Coupled assay of Na+,K+-ATPase activity. *Methods Enzymol.* **156**, 116–119 (1988).
27. S. H. Scheres, S. Chen, Prevention of overfitting in cryo-EM structure determination. *Nat. Methods* **9**, 853–854 (2012).
28. A. Rohou, N. Grigorieff, CTFFIND4: Fast and accurate defocus estimation from electron micrographs. *J. Struct. Biol.* **192**, 216–221 (2015).